

# Influence of Initial Surface Roughness on Severe Wear Volume for SUS304 Austenitic Stainless Steels

A. Kawamura, K. Ishida, K. Okada, T. Sato

**Abstract**—Simultaneous measurements of the curves for wear versus distance, wear rate versus distance, and coefficient of friction versus distance were performed *in situ* to distinguish the transition from severe running-in wear to mild wear. The effects of the initial surface roughness on the severe running-in wear volume were investigated. Disk-on-plate friction and wear tests were carried out with SUS304 austenitic stainless steel in contact with itself under repeated dry sliding conditions at room temperature. The wear volume was dependent on the initial surface roughness. The wear volume when the initial surfaces on the plate and disk had dissimilar roughness was lower than that when these surfaces had similar roughness. For the dissimilar roughness, the wear volume decreased with decreasing initial surface roughness and reached a minimum; it stayed nearly constant as the roughness was less than the mean size of the oxide particles.

**Keywords**—Austenitic stainless steel, initial surface roughness, running-in, severe wear.

## I. INTRODUCTION

STAINLESS steels are widely used for slide bearings in food and beverage manufacturing and processing industries because of their good corrosion resistance [1]. Martensitic stainless steel [2], surface-modified stainless steel [3], [4], and nitrogen-containing austenitic stainless steel [5] are used to reduce wear particles that mix in with food. However, these materials are very expensive. SUS304 stainless steel is cheap and has superior corrosion resistance. The hope is to improve the wear resistance of SUS304 stainless steel under dry sliding conditions at room temperature.

Adhesive wear of metals without lubricants under a light load at room temperature is classified as severe running-in wear or mild wear [6]. Severe running-in wear is larger for the wrong number of digits than mild wear [7]. Therefore, reducing the severe running-in wear volume is very important to improving the wear resistance.

This study investigated the wear-resistance improvement of SUS304 stainless steel in terms of the initial surface roughness against the severe running-in wear volume. Repeated dry sliding experiments on SUS304 stainless steel in contact with

itself at room temperature were carried out with disk-on-plate friction and wear testers. The severe–mild wear transition was judged *in situ* by simultaneous measurements of the wear depth versus sliding distance, wear depth rate versus sliding distance, and coefficient of friction versus sliding distance. SUS304 stainless steel in contact with itself was chosen because of accelerated adhesive wear tests [8].

## II. EXPERIMENTAL

Fig. 1 shows a general view of the friction and wear apparatus. Fig. 2 shows a schematic diagram of the friction and wear apparatus. Fig. 3 shows a detail diagram of the test specimens and wear depth  $D$  between a fixed plate and a rotated disk specimen. The load was applied to specimens from the bottom to the top by a lever system, as shown in Fig. 2. The disk diameter was 40mm, its thickness was 5mm, and the radius of curvature of the disk end face was 10mm. The plate dimensions were 30mm × 30mm × 5mm. Table I shows the test conditions. A laser displacement sensor with a measurement resolving power of 0.01 $\mu$ m and measurement accuracy of  $\pm 0.1\%$  was attached to the board at the same level as the rotating shaft of the tester as shown in Fig. 2, and the wear depth  $D$  between the plate and the disk was measured as shown in Fig. 3. The specimens were SUS304 austenitic stainless steel, as shown in Table II. A laser microscope with a plane measurement accuracy of 0.02 $\mu$ m, height measurement accuracy of 0.012 $\mu$ m, and cut-off value  $\lambda_s$  of 2.5 $\mu$ m was used to measure the surface roughness. The particle size distribution of the wear debris was measured by a laser scattering particle distribution analyzer that can measure particle diameters of 0.02–2000 $\mu$ m.

The specimens were finished with abrasive grinding sandpaper. Table III shows the maximum height roughness of the initial specimen surfaces. There were two combinations of initial surface roughness between the plate and disk: dissimilar and similar (Table III). For the dissimilar roughness group, plane specimens were finished with only P400 grit sandpaper, and disk specimens were finished with various P-scale grit sandpapers. For the similar roughness group, the plate and disk had the same initial surface roughness. The equivalent initial surface roughness  $Rz$  for the maximum roughness heights between the plane  $Rz1$  and the disk  $Rz2$  was calculated from the equation of the harmonic mean described in Table III. Fig. 4 shows the relation between  $Rz$  and the P-scale grit of the sandpaper. Fig. 4 shows that  $Rz$  became large as the P-scale grit of the sandpaper decreased. The specimen weight was measured with an electric balance. The specimen weight difference before and after the friction test was divided by the specific gravity for the wear volume.

A. Kawamura is a doctoral program student of Interdisciplinary Graduate School of Science and Technology, Shinshu University, Okaya, JP (phone: +81-266-23-8613; fax: +81-266-23-8613; e-mail: 11st203b@shinshu-u.ac.jp).

K. Ishida is with the Center for Creative Technology, University of Yamanashi, Kofu, JP (e-mail: isawa@yamanashi.ac.jp).

K. Okada is with the Department of Materials Science and Engineering, Shinshu University, Okaya, JP (e-mail: okada@shinshu-u.ac.jp).

T. Sato is with the Department of Electrical and Electronic Engineering, Faculty of Engineering, Shinshu University, Nagano, JP (e-mail: labyam1@shinshu-u.ac.jp).

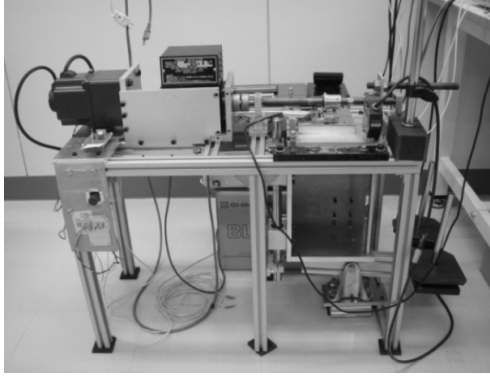


Fig. 1 General view of friction/wear apparatus

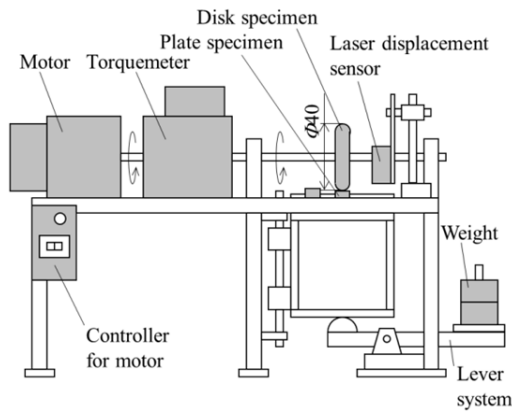


Fig. 2 Diagram of friction/wear apparatus

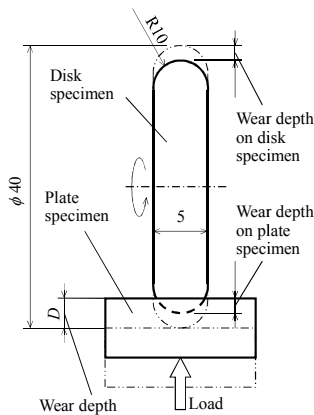

 Fig. 3 Detail diagram of specimens and wear depth  $D$ 

 TABLE I  
 FRICTION/WEAR TEST CONDITIONS

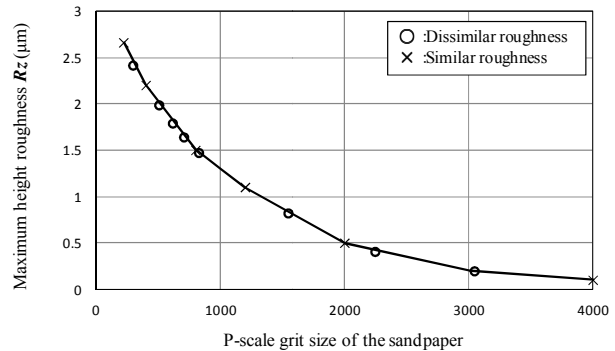
Specimen (Plate, Disk)	SUS304 (176HV)
Mean contact pressure (MPa)	290
Sliding velocity (m/s)	0.63
Rotational velocity (rpm)	300
Experimental temperature ( $^{\circ}$ C)	25
Relative humidity, (%)	20
Sampling frequency for measuring (Hz)	100
Atmosphere	In air

 TABLE II  
 CHEMICAL COMPOSITIONS (WT %)

Material	C	Si	Mn	P	S	Ni	Cr
SUS304	0.08	1.00	2.00	0.045	0.030	8.00-10.50	18.00-20.00

 TABLE III  
 SURFACE ROUGHNESS

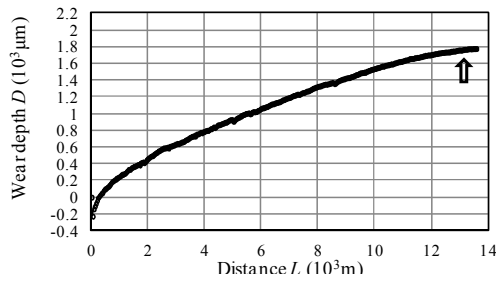
Specimen	Dissimilar roughness	Similar roughness
$R_z$ : Maximum height	Plate: $R_z1$ Disk: $R_z2$	2.2 2.7,1.8,1.5,1.3, 1.1,0.5,0.2,0.1
$R_z$ : Equivalent roughness $2/R_z=(1/R_z1)+(1/R_z2)$	Refer to Fig. 4	


 Fig. 4 Relation between maximum height roughness  $R_z$  and abrasive grinding P-scale grit size of the paper

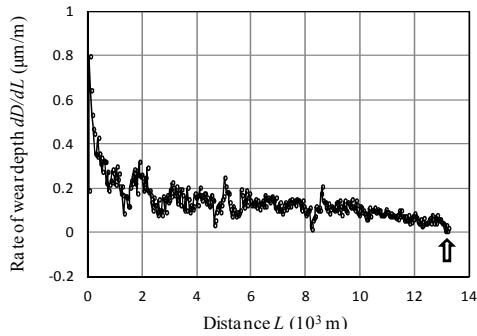
### III. RESULTS AND DISCUSSION

#### A. Distinguishing the Transition

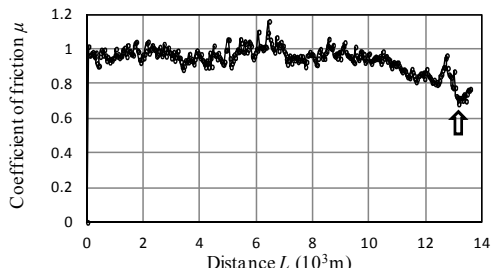
Generally, a wear depth curve that indicates the wear depth  $D$  as a function of sliding distance  $L$  changes smoothly. It is very difficult to exactly identify the severe–mild wear transition from only the wear depth curve. However, the wear depth rate  $dD/dL$  can be sensitively detected *in situ* by differentiating the wear depth of the  $D-L$  curve with respect to sliding distance  $L$ . In addition, a rapid decrease in the coefficient of friction takes place at the transition distance from the severe running-in wear to mild wear [9]. Therefore, the transition from severe running-in wear to mild wear might be precisely judged *in situ* from three curves: that is, wear depth of the  $D-L$  curve, wear depth rate of the  $dD/dL-L$  curve, and friction coefficient of the  $\mu-L$  curve. An example of the maximum height roughness  $R_z = 2.4\mu$ m is shown in Figs. 5 (a)–(c). The derivative of Fig. 5 (a) with respect to  $L$  is shown in Fig. 5 (b). The wear depth rate became approximately less than  $0.02\mu$ m/m at the sliding distance shown by the arrow in Fig. 5 (b). Note that the  $dD/dL-L$  curve may be much more effective than the  $D-L$  curve for identifying the transition from severe running-in wear to mild wear. The coefficient of friction reduced from 1.0 to 0.7 at the distance shown by the arrow in Fig. 5 (c). Based on *in situ* judgment of the results in Fig. 5, the severe–mild wear transition distance is approximately  $13.3 \times 10^3$  m, as shown by the arrows in Fig. 5.



(a) Wear depth as a function of sliding distance



(b) Rate of wear depth as a function of sliding distance



(c) Coefficient of friction as a function of sliding distance

Fig. 5 Wear and friction measurements, arrows indicate the severe-mild transition distance

**B. Running-in**

Fig. 6 shows the disk surface profiles of the wear tracks as obtained by the laser displacement sensor on the plate (1) and disk (2), respectively, just after the severe–mild wear transition in Fig. 5 occurred. The contour of the track is shown in (a1) and (a2). The surface roughness of (b1) and (b2) were taken as the horizontal track contour of (a1) and (a2) replaced the horizontal axis of (b1) and (b2), respectively. The enlarged smooth part of (b1) and (b2) are shown in (c1) and (c2), respectively. Figs. 6 (a1) and (a2) had the same contours, and roughness  $Rz$  in Figs. 6 (b1) and (b2) also had the approximate value. Skewness  $Ssk$  in Figs. 6 (b1) and (b2) had the same negative value. Thus, running-in was completed at the severe–mild wear transition distance indicated by the arrow in Fig. 5. Figs. 7 (a) and (b) show the wear track micrographs at the transition in Fig. 5 corresponding to Figs. 6 (1) and Figs. 6 (2), respectively. The smooth surface regions  $F_p$  in Fig. 7 (a) and  $F_d$  in Fig. 7 (b) may correspond to those in Figs. 6 (c1) and Figs. 6 (c2), respectively.

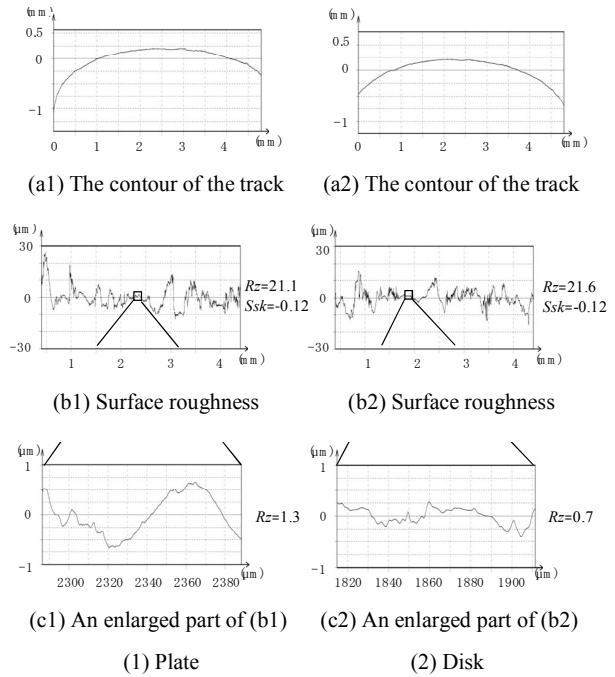


Fig. 6 Wear track profiles of the plate/disk perpendicular to the sliding direction just after the severe-mild transition occurred. Roughness (b) was taken as the horizontal contour of (a) replaced the horizontal axis of (b)

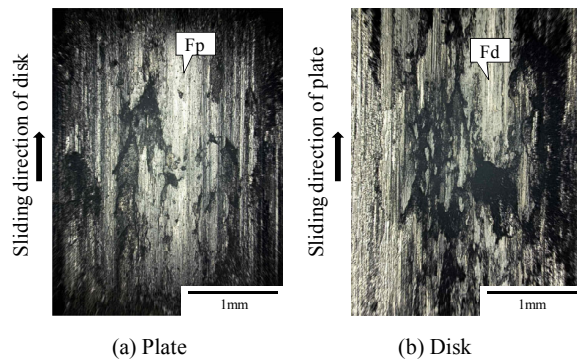


Fig. 7 Micrograph images of wear tracks just after the severe-mild transition occurred

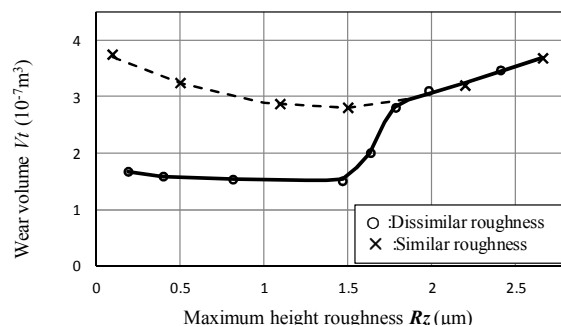


Fig. 8 Relation between wear volume  $V_t$  and maximum height roughness  $Rz$   
 ○: The initial surface on the plate and disk had dissimilar roughness  
 ×: The initial surface on the plate and disk had similar roughness

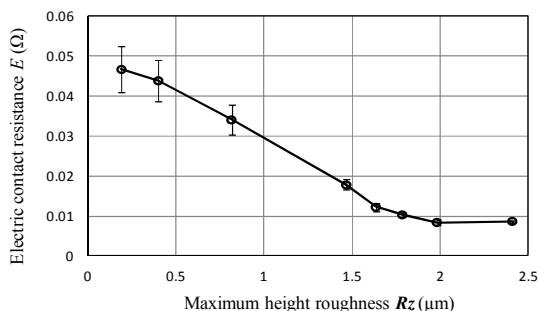


Fig. 9 Relation between electric contact resistance  $E$  and maximum height roughness  $R_z$  for the dissimilar roughness

### C. Initial Surfaces for the Dissimilar Roughness and Wear Volume

The full curve in Fig. 8 shows the relation between the wear volume and the maximum height roughness  $R_z$  of the initial specimen surfaces for the dissimilar roughness before sliding: (1) when  $R_z$  was larger than  $1.5\mu\text{m}$ , the wear volume decreased with decreasing initial surface roughness  $R_z$  and became lowest at  $R_z = 1.5\mu\text{m}$ ; (2) when  $R_z$  was less than  $1.5\mu\text{m}$ , the wear volume was nearly constant with respect to the initial surface roughness  $R_z$ ; and (3) the minimum wear volume for  $R_z = 1.5\mu\text{m}$  was about 40% of the wear volume when  $R_z = 2.4\mu\text{m}$ .

To clarify why  $V_i/R_z > 0$  in the full curve of Fig. 8 when  $R_z$  was larger than  $1.5\mu\text{m}$ ; the electric contact resistance was examined. Fig. 9 shows the relation between the electric contact resistance  $E$  and the initial surface roughness  $R_z$  for the dissimilar roughness.  $E$  decreased with increasing  $R_z$ . The decrease in  $E$  can be caused by the increase in real contact area [10]. This phenomenon may stimulate further adhesion and growth of transfer particles, which increases the wear volume.

To clarify why the wear volume was almost constant when  $R_z$  was less than  $1.5\mu\text{m}$  in the full curve of Fig. 8, wear particles were examined using a laser scattering particle analyzer and SEM and EDX, as shown in Figs. 10: (a1), (b1), and (c1) are metallic colored particles; (a2), (b2), and (c2) are black colored particles; (a1) and (a2) are the particle size distributions; (b1) and (b2) are SEM images; and (c1) and (c2) are EDX spectra.

Figs. 10 (a1), (b1), and (c1) show that metallic colored particles were rolled; their mean size was  $20\mu\text{m}$ , and most of the particles were not oxidized. The mean size of the metallic particles in Fig. 10 (a1) was nearly equal to the maximum height roughness  $R_z$  of the wear surfaces shown in both Fig. 6 (b1) and Fig. 6 (b2). Therefore, it is assumed that metallic particles can be produced at rough contact interfaces. This effect can increase the wear volume as the initial surface roughness is increased.

Fig. 10 (a2), (b2), and (c2) show that the mean size of black colored wear particles was divided into two groups:  $1.5$  and  $0.12\mu\text{m}$ . The black particles were oxides. The oxide particle size of  $1.5\mu\text{m}$  was nearly equal to the maximum height roughness  $R_z$  of the smooth surface, as shown in Figs. 6 (c1) and (c2). Therefore, it can be assumed that oxide particles can be produced at smooth interfaces. This effect can decrease the

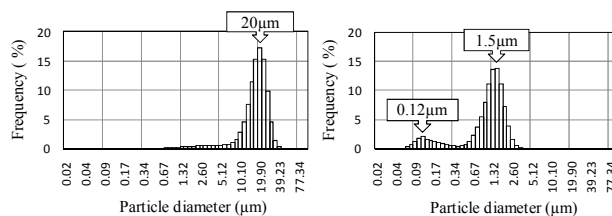
wear volume because oxide particles act as solid lubricants [11]. The  $1.5\mu\text{m}$  oxide particle size was the same as the initial surface roughness when the wear volume was the lowest, as shown in Fig. 8 for the full curve. The initial surface roughness can be assumed to stimulate further productive activity for the oxide particles, which decreases the wear.

The production mechanism of nanometer-sized oxide particles of  $0.12\mu\text{m}$ , as shown in Fig. 10 (a2), is not clear. However, it can be supposed that oxide particles with a size of  $1.5\mu\text{m}$  can aggregate at smooth micro-interfaces and crash into each other [12] to result in the production of nanometer-sized oxide particles. The smallest wear particle size was  $0.07\mu\text{m}$ , as shown in Fig. 10 (c2) [13].

### D. Similar and Dissimilar Roughness of Specimens

A series of experiments were performed, as shown by the broken curve of similar roughness in Fig. 8, to finish the plate and disk with the same P-scale grit sandpapers. Fig. 8 shows two results: the wear volume of the broken curve for similar roughness was larger than that of the full curve for dissimilar roughness, and the wear volume for the broken curve was at its minimum at the roughness of  $R_z = 1.5\mu\text{m}$ , which was nearly equal to the size of the oxide wear particle.

The effects of the oxide wear particle on wear volume were classified into two types: the solid lubricant effect [11], as discussed in the previous section; and the abrasive effect [14]. A low amount of oxide particles in the sliding interface can affect wear like a solid lubricant; these results in a decrease in wear volume. A large amount of oxide particles on the sliding interface can act on wear as an abrasive; these results in an increase in wear volume. Wear volume may also depend on the relative size of the oxide wear particles to the surface roughness of specimens. When the wear particle size is larger than the surface roughness of both specimens, the oxide wear particles that form can be sealed in smooth contact interfaces and act on wear as an abrasive with increased wear volume to decrease surface roughness. When the wear particle size is smaller than the surface roughness of both specimens, metallic wear particle formation may predominate over oxide wear particle formation with increased wear volume as the surface roughness increases. As a result, the wear volume for similar roughness, as shown by the broken curve in Fig. 8, reached its minimum when the size of the oxide wear particle corresponded to a roughness of  $R_z = 1.5\mu\text{m}$ .



(a1) Distribution of particle size

(a2) Distribution of particle size

(b1) SEM image

(b2) SEM image

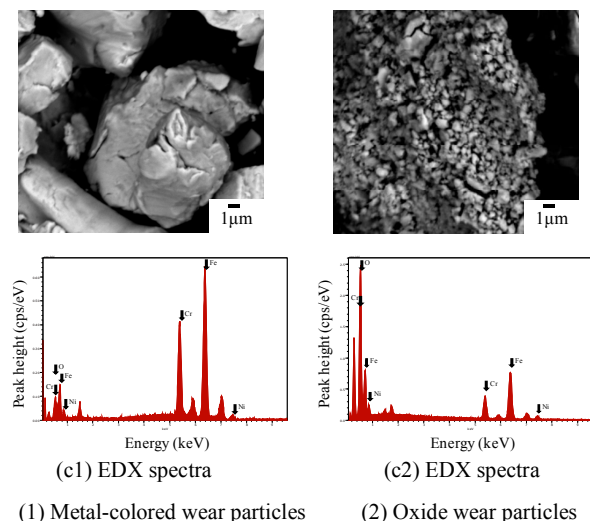


Fig. 10 Wear particles

When the surface roughness of either the plate or disk was larger than the wear particle size, the oxide wear particles may easily escape from the smooth contact interfaces to the rough contact interfaces; residual oxide wear particles on the smooth interfaces can act as lubricants to result in the broken curve of similar roughness over the full curve of dissimilar roughness shown in Fig. 8.

#### IV. CONCLUSION

Simultaneous experiments on the curves of wear depth versus distance, wear depth rate versus distance, and coefficient of friction versus distance were performed *in situ* to identify the transition from severe running-in wear to mild wear and clarify the effect of the initial surface roughness on severe running-in wear volume. A disk-on-plate friction and wear tester was used on SUS304 austenitic stainless steel in contact with itself under repeated dry sliding conditions at room temperature. The main results were as follows. (1) Severe running-in wear volume was dependent on the initial surface roughness: that is, the wear volume when the roughness of the initial surfaces of the plate and disk was dissimilar was lower than that when the roughness of the initial surfaces was similar. (2) For the dissimilar roughness, when the initial surface roughness was larger than  $1.5\mu\text{m}$ —that is, nearly equal to the oxide wear particle size—the wear volume decreased with decreasing initial surface roughness  $R_z$  and reached its minimum at  $R_z = 1.5\mu\text{m}$ ; when  $R_z$  was less than  $1.5\mu\text{m}$ , the wear volume stayed nearly constant with respect to the initial surface roughness. (3) The minimum wear volume for  $R_z = 1.5\mu\text{m}$  was about 40% of the wear volume for  $R_z = 2.4\mu\text{m}$ . And (4) three kinds of wear particles were observed—metallic particles with a mean size of  $20\mu\text{m}$  and oxide particles with mean sizes of  $1.5$  and  $0.12\mu\text{m}$ .

#### REFERENCES

[1] Luis. C. Sreabra, A. M. Bapista, "Tribological behavior of food grade polymers against stainless steel in dry sliding and with sugar," *Wear*, vol.253, 2002, pp. 394-402.

- [2] J. R. Laguna-Camacho, A. Marquina-Chavez, J. V. Mendez-Mendez, M. Vite-Torres, E. A. Gallardo-hernandez, "Solid particle erosion of AISI304, 316 and 420 stainless steels," *Wear*, Available online 16 January, 2013.
- [3] Y. Sun, T. Bell, "Dry sliding wear resistance of low temperature plasma carburized austenitic stainless steel," *Wear*, vol.253, 2002, pp. 689-693.
- [4] Zhao Cheng, C. X. Li, H. Dong, T. Bell, "Low temperature plasma nitrocarburising of AISI 316 austenitic stainless steel," *Surface and Coating Technology*, vol.191, 2005, pp. 195-200.
- [5] M. O. Speidel, "Nitrogen containing austenitic stainless steels," *Mat-wissa. a. Werkstofftech*, vol.37, no.10, 2006, pp. 875-880.
- [6] W. Hirst, J. K. Lancaster, "Surface film formation and metallic wear," *Journal of Applied Physics*, vol.27, 1956, pp. 1057-1065.
- [7] N. C. Welsh, "The dry wear of steels □. The general pattern of behavior," *Philosophical Transactions of the Royal Society of London. Series A*, vol.257, no.1077, 1965, pp. 31-50.
- [8] F. P. Bowden, D. Tabor, *The friction and lubrication of solids*, Clarendon press, Oxford, London, 1954, pp. 306-314.
- [9] S. M. Mahdavian, Y. W. Mai, B. Contrell, "Friction metallic transfer and debris analysis of sliding surfaces," *Wear*, vol.82, 1982, pp. 221-232.
- [10] M. Braunovic, N. K. Myshkin, V. Konchits, *Electrical contacts: fundamentals, applications and technology*, CRC Press, Danvers, MA, 2007, pp. 166-180.
- [11] H. Kato, "Severe-mild wear transition by supply of particles on sliding surface," *Wear*, vol.255, 2003, pp. 426-429.
- [12] I. M. Feng, B. G. Rightmire, "An experimental study of fretting," *Proceedings of the Institution of Mechanical Engineers*, vol.70, 1956, pp. 1055-1064.
- [13] E. Rabinowicz, *Friction and wear*, Jhon Willy and son, Inc, New York, 1965, pp. 125-166.
- [14] K. Hokkirigawa, K. Kato, "An experimental and theoretical investigation of ploughing, cutting and wedge formation during abrasive wear," *Tribology International*, vol.21, no.1, 1988, pp.51-57.

**Akira Kawamura** was born in Miyagi, JP, May 27 1950. B. A. in 1990, The Open University of Japan. Professional Engineer, Japan. APEC Engineer. M' of JSTP, and JAST.

**Kazuyoshi Ishida** was born in Aichi, JP, April 6 1975. B. S. Eng. in 1998, M. S. Eng. in 2000 and Ph.D. in 2006, Yamanashi University, Kofu, JP. Associate Prof. of University of Yamanashi, Kofu, JP. M' of JSLE and JSPE.

**Katsuzo Okadawas** born in Tokyo, JP, January 16 1945. B. S. Eng. in 1966 and M.S.Eng. in 1968, Yamanashi University. Kofu, JP. Ph.D. in 1980, Tokyo Institute of Technology, Tokyo, JP. Project professor of Shinshu University, Okaya, JP. Professor emeritus, University of Yanamashi, Kofu, JP. M' of JSLE and JSPE.

**Toshiro Sato** was born in Niigata, JP, April 12, 1959. B.S. Eng. in 1982, M. S. Eng. in 1984, Ph.D. in 1989, Chiba University, Chiba, JP. Professor of Shinshu University, Nagano, JP. M' of IEEEJ, MSJ, and IEEE Mag. Soc..